



# The Universal $\gamma$ -Ray Flux, Grand Unified Theories, and Extragalactic Magnetic Field

Günter Sigl<sup>1,2</sup>, Sangjin Lee<sup>1,2</sup>, and Paolo Coppi<sup>3</sup>

<sup>1</sup>*Department of Astronomy & Astrophysics  
Enrico Fermi Institute, The University of Chicago, Chicago, IL 60637-1433*

<sup>2</sup>*NASA/Fermilab Astrophysics Center  
Fermi National Accelerator Laboratory, Batavia, IL 60510-0500*

<sup>3</sup>*Department of Astronomy  
Yale University, New Haven, CT 06520-8101*

## ABSTRACT

The isotropic component of the  $\gamma$ -ray flux between 100 MeV and 100 EeV ( $10^{20}$  eV) contains important information about the origin of highest energy cosmic rays and the extragalactic magnetic field (EGMF). Using numerical simulations of extragalactic cosmic and  $\gamma$ -ray propagation we show that an average fraction of  $\simeq 10\%$   $\gamma$ -rays in the total cosmic ray flux around 10 EeV would imply both a non-acceleration origin of highest energy cosmic rays and a large scale EGMF  $\lesssim 10^{-11}$  G. Proposed observatories for ultrahigh energy cosmic rays should be able to test this signature.



# 1 Introduction

The highest energy cosmic ray (HECR) events observed above 100 EeV [1, 2] are difficult to explain within conventional models involving first order Fermi acceleration of charged particles at astrophysical shocks [3]. It is hard to accelerate protons and heavy nuclei up to such energies even in the most powerful astrophysical objects [4], like radio galaxies and active galactic nuclei. In addition, nucleons above  $\simeq 70$  EeV undergo photopion production on the cosmic microwave background (CMB), which is known as the Greisen-Zatsepin-Kuzmin (GZK) effect [5] and limits the distance to possible sources to less than  $\simeq 100$  Mpc [6]. Heavy nuclei are photodisintegrated in the CMB within a few Mpc [7].

Within “top-down” (TD) scenarios, in contrast, predominantly  $\gamma$ -rays and neutrinos are initially produced at ultrahigh energies (UHEs) by quantum mechanical decay of supermassive elementary X particles related to some grand unified theory (GUT). Such X particles could be released from topological defect relics of phase transitions which might have been caused by spontaneous breaking of GUT symmetries in the early universe [8]. Since the absolute flux level predicted by TD models is very model dependent [9], we will allow an arbitrary flux normalization noting that certain TD scenarios such as annihilation of magnetic monopole-antimonopole pairs [10] yield HECR fluxes consistent with observations. Such models are attractive in explaining HECRs because they predict injection spectra which are considerably harder than shock acceleration spectra and, unlike the GZK effect for nucleons, there is no threshold effect in the attenuation of UHE  $\gamma$ -rays which dominate the predicted flux.

Above 100 EeV, signatures for TD scenarios, based on spectral features such as a “gap” [11], and on the  $\gamma$ -ray to total cosmic ray ( $\gamma$ /CR) flux ratio [12] have been suggested. In this letter, we explore alternative signatures, based on the isotropic component of the  $\gamma$ -ray flux below 100 EeV, particularly around 10 EeV, by applying detailed numerical simulations of extragalactic cosmic and  $\gamma$ -ray propagation [13]. The exposure required to test this signature is significantly smaller than for measurements above 100 EeV, as long as discrimination between  $\gamma$ -rays and charged cosmic rays (CRs) is possible at a level of a few percent. This is within reach of proposed experiments [14].

## 2 Top-Down Models

Topological defects from phase transitions in the early universe such as cosmic strings, monopoles, and domain walls are topologically stable, but nevertheless can release part of their energy via collapse or annihilation in the form of X particles. The X particles can be gauge bosons, Higgs bosons, superheavy fermions, etc. depending on the specific GUT, their mass  $m_X$  being comparable to the symmetry breaking scale. They subsequently typically decay into a lepton and a quark which roughly share the initial energy equally. The quark then hadronizes into nucleons ( $N$ s) and pions, the latter ones in turn decaying into  $\gamma$ -rays, electrons, and neutrinos. Given the X particle injection rate,  $dn_X/dt$ , the effective injection

spectrum of particle species  $a$  ( $a = \gamma, N, e^\pm, \nu$ ) can be written as

$$\Phi_a(E, t) = \frac{dn_X}{dt} \frac{2}{m_X} \frac{dN_a}{dx} \quad (1)$$

where  $x \equiv 2E/m_X$ , and  $dN_a/dx$  is the relevant effective fragmentation function. We take the primary lepton to be an electron injected with energy  $m_X/2$ . The total hadronic fragmentation function  $dN_h/dx$  is in principle determined by quantum chromodynamics (QCD) and, in the relevant energy range, may be taken as [15]

$$\frac{dN_h}{dx} = \frac{15}{16} x^{-3/2} (1-x)^2 \quad \text{for } x \leq 1. \quad (2)$$

We assume that about 3% of the total hadronic content consists of nucleons and the rest is produced as pions and distributed equally among the three charge states. The standard pion decay spectra then determine the injection spectra of  $\gamma$ -rays, electrons, and neutrinos. The  $X$  particle injection rate is assumed to be spatially uniform and in the matter-dominated era can be parametrized as [8]

$$\frac{dn_X}{dt} \propto t^{-4+p}, \quad (3)$$

where  $p$  depends on the specific defect scenario. In this letter we focus on the case  $p = 1$  which is representative for a network of ordinary cosmic strings [16] and annihilation of monopole-antimonopole pairs [10].

### 3 Numerical Simulations

Injection of high energy  $\gamma$ -rays and electrons generate electromagnetic (EM) cascades on the low energy radiation fields such as the CMB. High energy photons undergo electron-positron pair production (PP;  $\gamma\gamma_b \rightarrow e^-e^+$ ). In the Klein-Nishina regime where the squared center of mass energy is large compared to the squared electron mass, one particle usually carries almost all the initial energy. This “leading” electron (positron) in turn can transfer almost all of its energy to a background photon via inverse Compton scattering (ICS;  $e\gamma_b \rightarrow e'\gamma$ ). EM cascades are driven by this cycle of PP and ICS. The energy degradation of the “leading” particle in this cycle is rather slow, whereas the total number of particles grows exponentially with time. This makes a standard Monte Carlo treatment difficult. We therefore solve the relevant kinetic equations implicitly which allows us to deal with the very different length scales involved. Our numerical solutions fully account for all produced particles, whereas the often used continuous energy loss (CEL) approximation [12] takes into account only the leading particles in the cascade and thus underestimates the flux at lower energies for a cascade that is not fully developed. A detailed account of our transport equation approach for  $\gamma$ -ray propagation is found in Ref. [13]. We include all EM interactions that influence the  $\gamma$ -ray spectrum in the energy range  $10^8 \text{ eV} < E < 10^{25} \text{ eV}$ , namely PP, ICS, triplet pair production (TPP;  $e\gamma_b \rightarrow ee^-e^+$ ), and double pair production ( $\gamma\gamma_b \rightarrow e^-e^+e^-e^+$ ). The

relevant nucleon interactions implemented are pair production by protons ( $p\gamma_b \rightarrow pe^-e^+$ ), photoproduction of single or multiple pions ( $N\gamma_b \rightarrow N n\pi$ ,  $n \geq 1$ ), and neutron decay. Production of secondary  $\gamma$ -rays, electrons, and neutrinos by pion decay are also taken into account. We assume a flat, cosmological constant free universe and a Hubble constant of  $H_0 = 75 \text{ km sec}^{-1}\text{Mpc}^{-1}$  throughout.

The universal infrared and optical (IR/O) background strongly affects  $\gamma$ -ray propagation below  $\sim 10^{14}$  eV via pair production. The universal radio background (URB) affects UHE  $\gamma$ -rays above the pair production threshold at  $\sim 100$  EeV. Our numerical simulations account for the URB, the CMB, and the IR/O backgrounds, including their evolution with redshift [13]. For EGMF strengths  $\gtrsim 10^{-10}$  G, electrons above  $\simeq 100$  EeV lose energy effectively instantaneously through synchrotron radiation [17] which inhibits cascade development at these energies. The observed UHE  $\gamma$ -ray flux then mainly depends on the absorption length due to pair production.

## 4 Results

Fig. 1 shows the results for the  $\gamma$ -ray and nucleon fluxes from a typical TD scenario, assuming a negligible EGMF, along with current observational constraints on the  $\gamma$ -ray flux. The spectrum was normalized in the best possible way to allow for an explanation of the observed HE CR events (the flux below a few tens of EeV is presumably caused by conventional acceleration). Since the comparatively large amount of energy injected at high redshifts is recycled to lower energy  $\gamma$ -rays, TD models are significantly constrained [18, 19] by current limits on the diffuse  $\gamma$ -ray background in the 100 MeV – 10 GeV region [20, 21, 22]. Note that the IR/O background strongly depletes the  $\gamma$ -ray flux in the range  $10^{11} - 10^{14}$  eV, recycling it to energies below 10 GeV (see Fig. 1). The size of this effect is not very sensitive to the specific IR/O background model [24]. Constraints from limits on CMB distortions and light element abundances from  $^4\text{He}$ -photodisintegration are comparable to the bound from the directly observed  $\gamma$ -rays [19].

We first note that the scenario in Fig. 1 obeys all current constraints within the normalization ambiguities. This is in contrast to a recent claim [25] that TD models of HE CR origin might be ruled out altogether. Their conclusion only applies to the less realistic case of discrete sources of monoenergetic  $\gamma$ -ray and nucleon injection [13, 26].

Whereas the UHE nucleon and  $\gamma$ -ray fluxes are independent of cosmological evolution, the  $\gamma$ -ray flux below  $\simeq 10^{11}$  eV is proportional to the total energy injection which, for all other parameters held fixed, increases with decreasing  $p$  [19]. For  $m_X = 10^{23}$  eV, scenarios with  $p \lesssim 1$  are therefore ruled out (see Figs. 1 and 2), whereas constant comoving injection rates ( $p = 2$ ) are well within the limits. Since the EM flux above  $\simeq 10^{22}$  eV is efficiently recycled to lower energies, this constraint turns out to be basically independent of  $m_X$  in case of a vanishing EGMF [26], in contrast to earlier analytical estimates based on the CEL approximation which underestimates the flux around 100 EeV [18, 19].

Fig. 2 shows results for the same TD scenario as in Fig. 1, but assumes an EGMF of  $10^{-9}$  G which is near its currently believed upper limit [27]. The normalization of the injection

spectrum has been increased so that the observed UHE  $\gamma$ -ray and CR flux is consistent with the data. This leads to an increase of the predicted low energy  $\gamma$ -ray background by about a factor of 5 compared to the case of a negligible EGMF (see Fig. 1). The constraints from the flux limits below 10 GeV thus become somewhat tighter.

We now turn to signatures of TD models at UHEs. First note that in the scenario of Fig. 1 the full cascade calculation predicts  $\gamma$ -ray fluxes around 100 EeV that are about an order of magnitude higher than predictions by the often used CEL approximation. This shows the importance of non-leading particles in the development of unsaturated EM cascades. In a situation similar to the one in Fig. 1, Ref. [12] predicts a  $\gamma$ /CR flux ratio at 10 EeV of  $\simeq 8 \times 10^{-3}$  for an URB similar to the one used by us [28] and for the best possible normalization to the data. In contrast, our numerical calculation predicts  $\simeq 6 \times 10^{-2}$  for this ratio, about a factor of 7 higher. In addition, for an EGMF  $\lesssim 10^{-11}$  G, our results suggests a domination of  $\gamma$ -rays down to  $\simeq 60$  EeV (see Fig. 1) where Ref. [12] still predicts a domination by nucleons.

Based on current data, the experimental exposure required to detect one event in an energy bin centered around  $E = 300$  EeV whose width  $\Delta E$  is given by  $\log_{10}(\Delta E/E) = 0.1$  is  $\simeq 3 \times 10^{20}$  cm<sup>2</sup>secsr. In contrast, in the scenario of Fig. 1, the exposure required to detect one photon event in an energy bin of the same logarithmic width centered around  $E = 10$  EeV is about one order of magnitude smaller. These exposures are well within reach of the proposed Pierre Auger Cosmic Ray Observatories [14], which may be able to detect a neutral CR component down to a level of 1% of the total flux.

In contrast, if the EGMF strength is larger than  $\sim 10^{-11}$  G, cascade development is essentially inhibited and the UHE  $\gamma$ -ray spectrum is suppressed significantly (see Fig. 2). If the nucleon component from the TD model is normalized to the total CR flux at  $\simeq 5 \times 10$  EeV as was done in Fig. 2, the  $\gamma$ /CR flux ratio at 10 EeV is  $\simeq 4 \times 10^{-3}$  for an EGMF strength of  $\simeq 10^{-9}$  G. This is significantly lower than in case of a vanishing EGMF.

Another not well known factor affecting UHE  $\gamma$ -ray propagation is the URB for which we used the spectrum suggested in Ref. [28]. A higher overall amplitude reduces the  $\gamma$ -ray flux by a corresponding factor without changing its spectral shape. Thus, as long as the  $\gamma$ -ray flux dominates the nucleon flux in the TD component above  $\simeq 100$  EeV and the total flux is normalized to the HECR events, predictions for the  $\gamma$ /CR flux ratio below  $\simeq 100$  EeV are essentially independent of the URB amplitude and the hadronic fraction at injection. An URB cutoff frequency lower than 2 MHz (the value adopted in our analysis) affects this ratio in a less trivial way with a tendency to smaller values.

Fig. 3 shows typical spectra resulting from a uniform distribution of shock acceleration sources. This scenario leads to a UHE CR spectrum with a GZK cutoff and  $\gamma$ -rays are only produced as secondaries. Our treatment of multiple pion production by nucleons leads to secondary  $\gamma$ -ray fluxes somewhat higher than in Refs. [25, 29]. Note that the (isotropic)  $\gamma$ /CR flux ratio is  $\lesssim 10^{-3}$  at 10 EeV, much smaller than predictions by TD models for a small EGMF. Ratios as high as 10% can only be reached in the direction of powerful nearby acceleration sources which thereby might provide a means to “measure” the EGMF [17]. The secondary  $\gamma$ -ray flux generally decreases still further with decreasing maximum injection

energy and increasing EGMF [17].

## 5 Conclusions

Some TD type scenarios of HECR origin are still unconstrained by current data and bounds on  $\gamma$ -ray and UHE CR fluxes. For example, in case of an EGMF  $\ll 10^{-12}$  G, spatially uniform annihilation of magnetic monopoles and antimonopoles is still a viable model for GUT scales up to  $10^{16}$  GeV. A solid angle averaged  $\gamma$ /CR flux ratio at the 10% level at  $\simeq 10$  EeV is a signature of a non-acceleration origin of HECRs hinting to the presence of a TD mechanism. At the same time it would put an independent new upper limit of  $\simeq 10^{-11}$  G on the poorly known EGMF on scales of a few to tens of Mpc. Absence of a  $\gamma$ -ray flux at that level, on the other hand, may be explained either by a TD scenario with an EGMF strength  $\gtrsim 10^{-11}$  G or by a shock acceleration model. The test of this signature should be possible with currently proposed experiments. TD models also predict significant neutrino fluxes. Implications of this will be considered in a separate publication [26].

## Acknowledgments

We thank D. N. Schramm, J. W. Cronin, Chris Hill, and F. A. Aharonian for stimulating discussions and Shigeru Yoshida for comments. This work was supported by DOE, NSF and NASA at the University of Chicago, by the DOE and by NASA through grant NAG5-2788 at Fermilab, and by the Alexander-von-Humboldt Foundation. SL gratefully acknowledges the support of the POSCO Scholarship Foundation in Korea.

## References

- [1] D. J. Bird *et al.*, Phys. Rev. Lett. **71**, 3401 (1993); Astrophys. J. **424**, 491 (1994); *ibid.* **441**, 144 (1995).
- [2] N. Hayashida *et al.*, Phys. Rev. Lett. **73**, 3491 (1994); S. Yoshida *et al.*, Astropart. Phys. **3**, 105 (1995).
- [3] for a review see, e.g., R. Blandford and D. Eichler, Phys. Rep. **154**, 1 (1987).
- [4] A. M. Hillas, Ann. Rev. Astron. Astrophys. **22**, 425 (1984).
- [5] K. Greisen, Phys. Rev. Lett. **16**, 748 (1966); G. T. Zatsepin and V. A. Kuzmin, Pisma Zh. Eksp. Teor. Fiz. **4**, 114 (1966) [JETP. Lett. **4**, 78 (1966)].
- [6] G. Sigl, D. N. Schramm, and P. Bhattacharjee, Astropart. Phys. **2**, 401 (1994).
- [7] J. L. Puget, F. W. Stecker, and J. H. Bredekamp, Astrophys. J. **205**, 638 (1976).

- [8] P. Bhattacharjee, C. T. Hill, and D. N. Schramm, *Phys. Rev. Lett.* **69**, 567 (1992).
- [9] A. J. Gill and T. W. B. Kibble, *Phys. Rev. D* **50**, 3660 (1994).
- [10] P. Bhattacharjee and G. Sigl, *Phys. Rev. D* **51**, 4079 (1995).
- [11] G. Sigl, S. Lee, D. N. Schramm, and P. Bhattacharjee, *Science* **270**, 1977 (1995).
- [12] F. A. Aharonian, P. Bhattacharjee, and D. N. Schramm, *Phys. Rev. D* **46**, 4188 (1992).
- [13] S. Lee, submitted to *Phys. Rev. D*.
- [14] M. Boratav *et al.*, eds., *Nucl. Phys. B (Proc. Suppl.)* **28B** (1992).
- [15] C. T. Hill, *Nucl. Phys. B* **224**, 469 (1983).
- [16] P. Bhattacharjee and N. C. Rana, *Phys. Lett. B* **246**, 365 (1990).
- [17] S. Lee, A. V. Olinto, and G. Sigl, *Astrophys. J.* **455**, L21 (1995).
- [18] X. Chi *et al.*, *Astropart. Phys.* **1**, 129 (1993); *ibid.* **1**, 239 (1993).
- [19] G. Sigl, K. Jedamzik, D. N. Schramm, and V. Berezhinsky, *Phys. Rev. D* **41**, 342 (1990).
- [20] S. W. Digel, S. D. Hunter, and R. Mukherjee, *Astrophys. J.* **441**, 270 (1995).
- [21] C. E. Fichtel *et al.*, *Astrophys. J.* **217**, L9 (1977).
- [22] J. L. Osborne, A. W. Wolfendale, and L. Zhang, *J. Phys. G* **20**, 1089 (1994).
- [23] A. Karle *et al.*, *Phys. Lett. B* **347**, 161 (1995).
- [24] F. Aharonian and P. Coppi, in preparation.
- [25] R. J. Protheroe and P. A. Johnson, to appear in *Astropart. Phys.*
- [26] G. Sigl, S. Lee, and P. Coppi, in preparation.
- [27] P. P. Kronberg, *Rep. Prog. Phys.* **57**, 325 (1994).
- [28] T. A. Clark, L. W. Brown, and J. K. Alexander, *Nature* **228**, 847 (1970).
- [29] S. Yoshida and M. Teshima, *Prog. Theor. Phys.* **89**, 833 (1993).

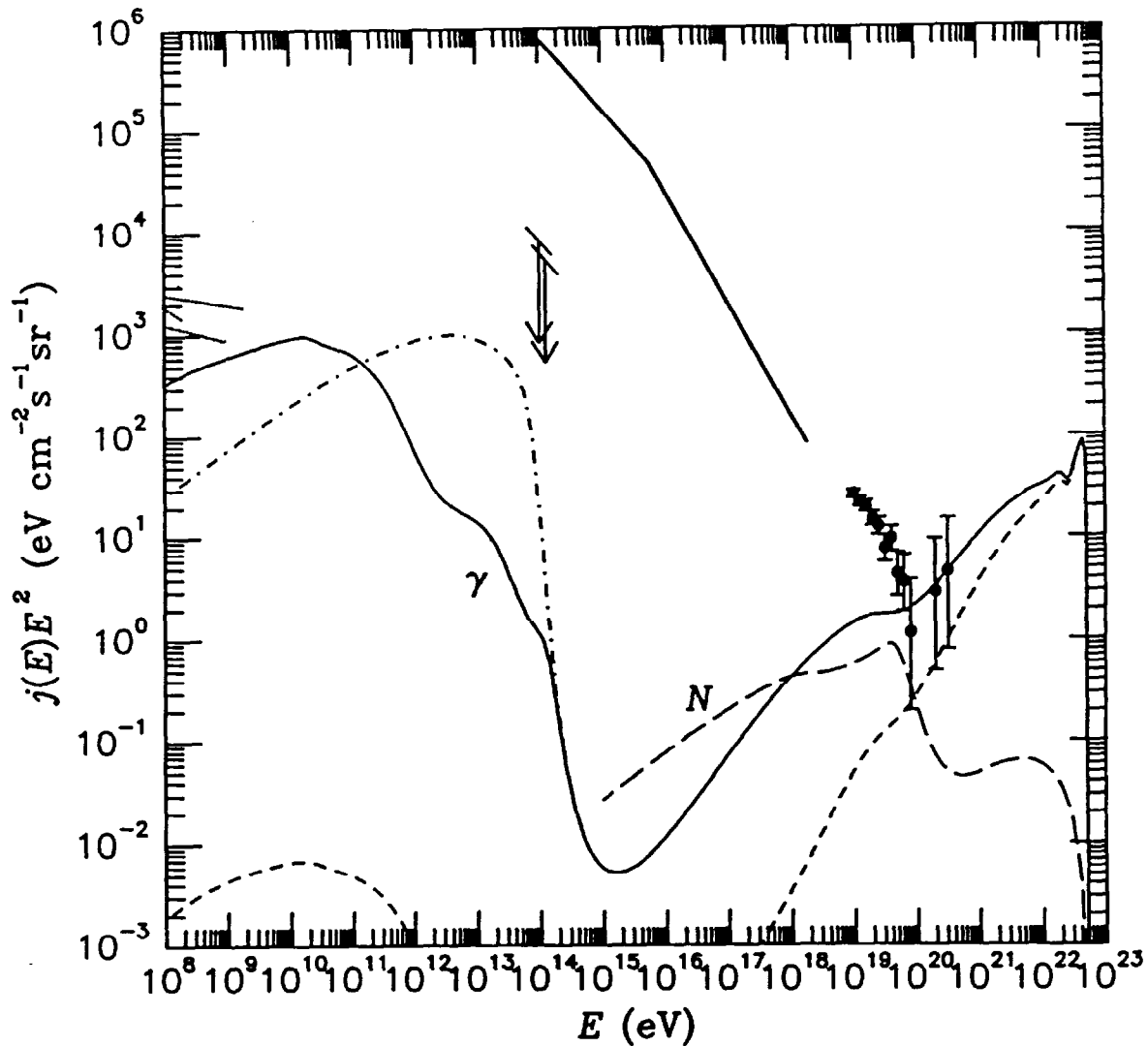


Figure 1: Predictions for the differential fluxes of  $\gamma$ -rays (solid line) and nucleons above  $10^{15}$  eV (long dashed line) by the TD model characterized by Eqs. (1) to (3) with  $p = 1$ ,  $m_X = 10^{23}$  eV, assuming a vanishing EGMF. The dashed line shows the  $\gamma$ -ray flux predicted by the CEL approximation. The dash-dotted line is for the case where the IR/O background is omitted. Also shown are the combined data from the Fly's Eye [1] and the AGASA [2] experiments above 10 EeV (dots with error bars), piecewise power law fits to the observed charged CR flux (thick solid line) and experimental upper limits on the  $\gamma$ -ray flux below 10 GeV from Refs. [20, 21, 22] (dotted lines on left margin in decreasing order). The arrows indicate limits on the  $\gamma$ -ray flux from Ref. [23].



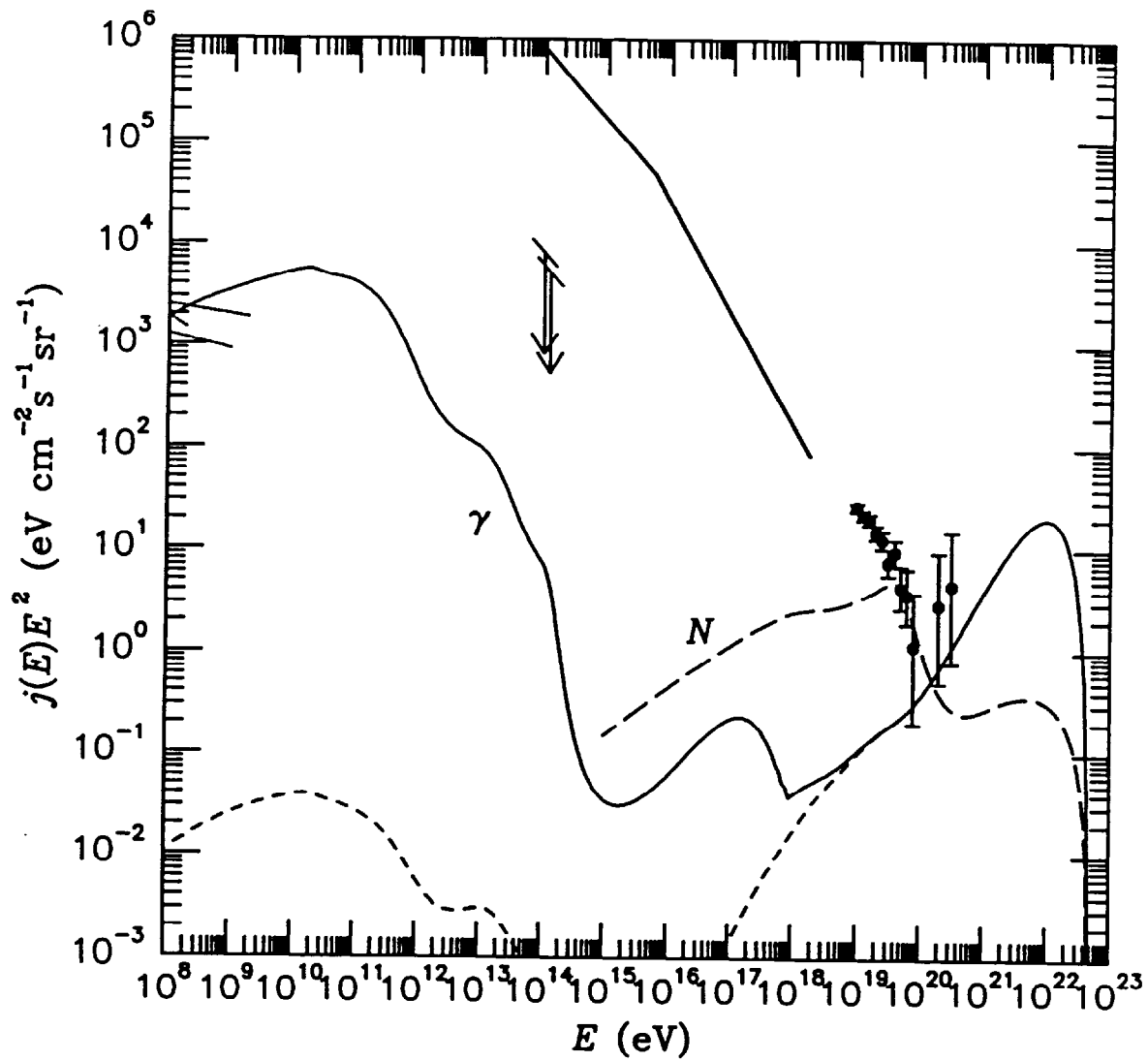


Figure 2: Same as Fig. 1, but for an EGMF of  $10^{-9}$  G. The results for a neglected IR/O background are not shown here.

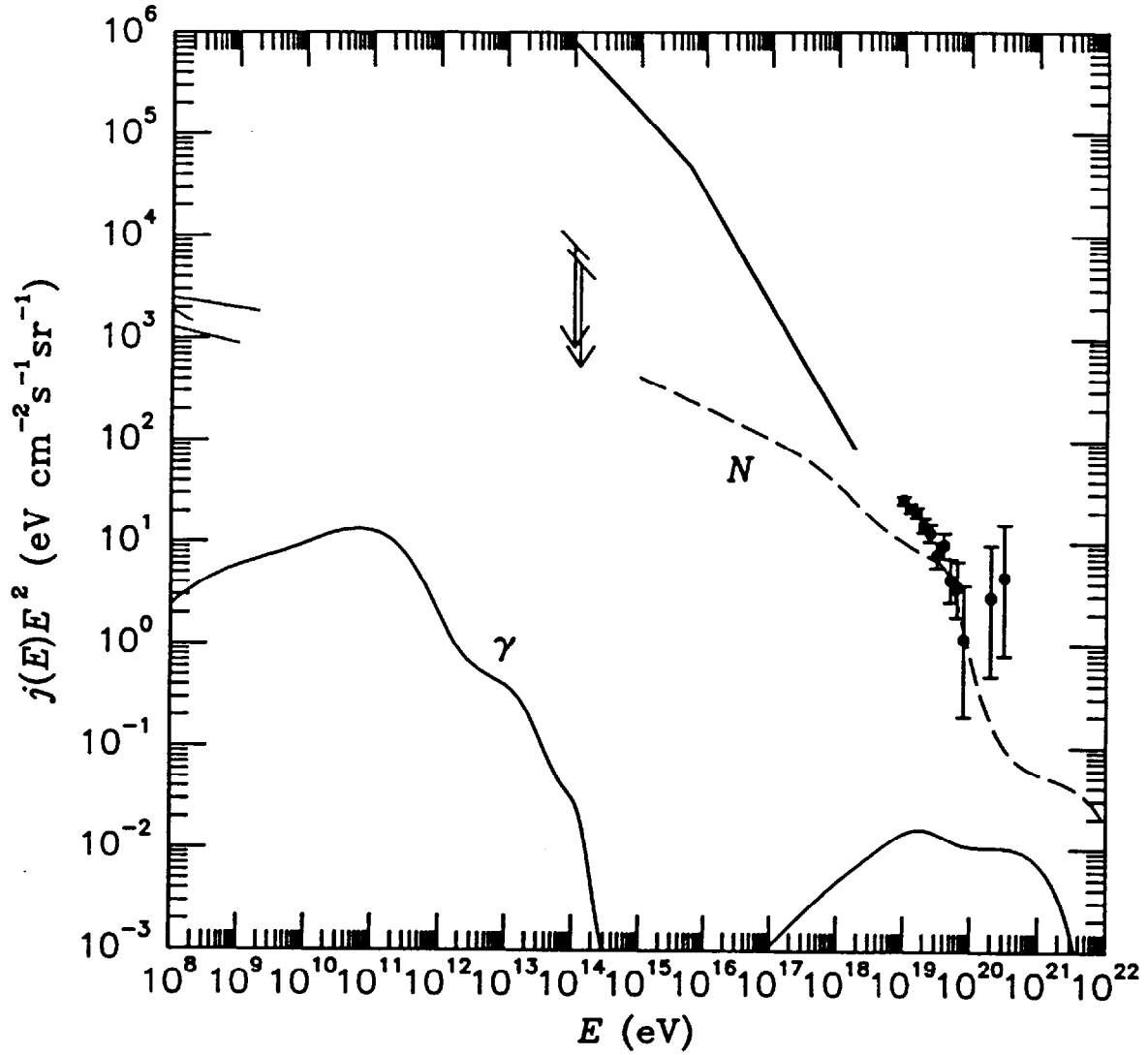


Figure 3: Predictions for the differential fluxes of  $\gamma$ -rays (solid line) and nucleons above  $10^{15}$  eV (long dashed line) by a uniform, constant comoving distribution of shock acceleration sources up to a redshift of 4, injecting protons with a spectrum  $\propto E^{-2.3}$  up to  $10^{22}$  eV, for a vanishing EGMF.